Sensitization of $NaMO_3$ (M: Nb and Ta) Photocatalysts with Wide Band Gaps to Visible Light by Ir Doping

Akihide Iwase, Kenji Saito, and Akihiko Kudo*

Department of Applied Chemistry, Faculty of Science, Tokyo University of Science,
1-3 Kagurazaka, Shinjuku-ku, Tokyo 162-8601

Received November 13, 2008; E-mail: a-kudo@rs.kagu.tus.ac.jp

$NiO/NaNbO_3$ (BG: 3.5 eV) showed photocatalytic activity for water splitting into H_2 and O_2 under UV irradiation. When $NaMO_3$ (M: Nb and Ta) was codoped with iridium ions and alkaline earth metal ions or lanthanum ions, a new visible-light absorption band was observed in addition to the band gap absorption band of the host material. The codopants of alkaline earth metal and lanthanum ions contributed to maintaining the charge balance and forming of fine crystals of the $NaMO_3$ powder. These $NaNbO_3$ and $NaTaO_3$ codoped with iridium ions and alkaline earth metal ions or lanthanum ions showed photocatalytic activities for H_2 or O_2 evolution from an aqueous solution containing a sacrificial reagent under visible light irradiation.

Development of visible-light-driven photocatalysts has been extensively studied in terms of effective utilization of solar energy. The doping of a foreign element is one of the strategies for this purpose.[1,2] The authors have reported TiO_2:Ni/Ta,[3] TiO_2:Cr/Sb,[4] and TiO_2:Rh/Sb[5] photocatalysts for O_2 evolution, and $SrTiO_3$:Rh,[6] $SrTiO_3$:Ir,[6] and $SrTiO_3$:Cr/Ta[7] photocatalysts for H_2 evolution in the presence of sacrificial reagents under visible light irradiation. These photocatalytic reactions proceed accompanied by electronic transitions from electron donor levels formed from partially filled d orbitals of Ni, Cr, Rh, and Ir ions to conduction bands composed of Ti3d orbitals of TiO_2 and $SrTiO_3$. The codopants of Ta and Sb keep the charge balance without formation of undesireble electron donor/acceptor levels in the forbidden band. Among doped metal oxide photocatalysts for H_2 evolution, $SrTiO_3$:Ir responds to visible light with longer wavelength than $SrTiO_3$:Rh and $SrTiO_3$:Cr/Ta. This result motivates us to study sensitization of wide band gap photocatalysts to visible light by Ir doping.

TiO_2 and $SrTiO_3$ are mainly employed as host materials for doping as mentioned above. However, the conduction bands of these materials have small driving forces for reduction of H_2O to form H_2. Therefore, the authors have focused on niobate and tantalate photocatalysts as the hosts because these materials generally have higher conduction band levels than titanates. Many niobate and tantalate photocatalysts for water splitting into H_2 and O_2 under UV irradiation have been reported.[2] Especially, $NaTaO_3$ photocatalysts doped with lanthanum or alkaline earth metal ions show high activity for overall water splitting.[8,9]

In the present study, photocatalytic properties of non-doped and Ir-doped $NaMO_3$ (M: Nb and Ta) were investigated to develop new visible-light-driven photocatalysts. Codoping effects on photocatalytic properties and the origin of visible light response are discussed.

Experimental

Powders of $NaMO_3$ (M: Nb and Ta) codoped with x mol % of Ir to M sites and y mol % of lanthanum or alkaline earth metal to Na sites were prepared by a solid-state reaction. The resulting materials are denoted as $NaMO_3$:Ir(x%)/A(y%). Starting materials, Na_2CO_3 (Kanto Chemical; 99.5%), Ta_2O_5 (Rare metallic; 99.99%), $SrCO_3$ (Kanto Chemical; 99.9%), $BaCO_3$ (Kanto Chemical; 99%), La_2O_3 (Kanto Chemical; 99.99%), and IrO_2 (Soekawa Chemical; 85.5% as Ir) were mixed in a ratio of Na:A:M:Ir $= 1.05{:}y{:}1{:}x$. The excess amount of sodium was added in the starting materials to compensate volatilization. For non-doped $NaNbO_3$ ($x = y = 0$), the mixture of starting materials was calcined at 973 K in air for 11 h in a platinum crucible. For Ir-doped $NaMO_3$, the mixture was calcined at 1173 K in air for 1 h and then 1423 K for 10 h in an alumina crucible. The excess sodium was washed out with water after the calcination. The crystal phase of obtained powder was confirmed by X-ray diffraction (Rigaku; MiniFlex). NiO-cocatalyst was loaded by impregnation and was subsequently pre-treated (H_2 reduction at 773 K for 2 h and O_2 oxidation at 473 K for 1 h) according to previous reports.[10,11]

Photocatalytic reactions were carried out in a gas-tight circulation system. The photocatalyst powder (0.3 g) was dispersed in water (350 mL) for overall water splitting into H_2 and O_2. An inner irradiation reaction cell made of quartz equipped with a 400-W high-pressure Hg lamp (SEN; HL400EH-5) was employed. The half reactions of water splitting that were H_2 evolution from an aqueous CH_3OH solution and O_2 evolution from an aqueous $AgNO_3$ solution were also examined using a top-irradiation reaction cell with a Pyrex window and a 300-W Xe lamp (Parkin-Elmer, CERMAX LX-300BUV). The wavelength of incident light was controlled with cutoff filters (Kenko). The amounts of evolved H_2 and O_2 were determined with gas chromatography (TCD, MS-5A, Ar carrier gas). Diffuse reflectance spectra were obtained using a UV–vis–NIR spectrometer (JASCO; Ubest-570) and were converted from reflection to absorbance by the Kubelka–Munk method. The photocatalyst powders were observed using a scanning electron microscope (Jeol; JSM-6700F).

Published on the web April 11, 2009; doi:10.1246/bcsj.82.514

Results and Discussion

Perovskite structure is a suitable crystal structure of photocatalysts for water splitting, as seen in $SrTiO_3$ and $NaTaO_3$.[2,8–11] However, there are few reports of photocatalytic water splitting over niobates with a simple perovskite structure, although many tantalates are active as represented by $NaTaO_3$. It is reported that $NaNbO_3$ prepared by a polymerized complex method shows activity for water splitting with the assistance of a RuO_2 cocatalyst.[12] The photocatalytic activity decreases with the reaction time and the amount of evolved O_2 is apart from stoichiometry. We examined photocatalytic water splitting over non-doped $NaNbO_3$ with a 3.5 eV band gap as shown in Figure 1. The $NaNbO_3$ powder was prepared by a solid-state reaction. The pretreated NiO(0.5 wt %)/$NaNbO_3$ was active for water splitting under UV irradiation. The activity was quite stable.

The sensitization of $NaMO_3$ (M: Nb and Ta) photocatalysts to visible light by Ir doping was explored. X-ray diffraction patterns of $NaMO_3$:Ir/A (A: Sr, Ba, and La) were the same as those of non-doped $NaMO_3$. It indicated that iridium ions, alkaline earth metal ions, and lanthanum ions were homogeneously doped into the $NaMO_3$ lattices. It was considered that iridium ions were substituted for M^{5+} sites, and alkaline earth metal and lanthanum ions were substituted for Na^{+} sites, judging from the ionic radii; Sr^{2+}: 1.58 Å, Ba^{2+}: 1.75 Å, La^{3+}: 1.50 Å, and Na^{+}: 1.53 Å for 12 coordination and Ir^{3+}: 0.82 Å, Ir^{4+}: 0.77 Å, Nb^{5+}: 0.88 Å, and Ta^{5+}: 0.88 Å for 6 coordination.[13]

Figure 2 shows SEM images of $NaMO_3$:Ir (M: Nb and Ta) with and without codoping of strontium and lanthanum. The particle sizes of Ir- and A-codoped $NaMO_3$ were one order of magnitude smaller than those of $NaMO_3$ doped with only Ir. Fine particles were also obtained for $NaMO_3$ with a barium codopant, being similar to $NaTaO_3$ doped with lanthanum and alkaline earth metal ions.[8,9]

Figure 3 shows diffuse reflectance spectra of $NaMO_3$:Ir/A (M: Nb and Ta, A: Sr and La) with and without H_2-reduction. $NaMO_3$:Ir had new absorption bands in the visible light region in addition to the band gap absorption bands of the $NaMO_3$ hosts. Although stable oxidation numbers of iridium are generally trivalent or tetravalent, Ir^{4+} is stable rather than Ir^{3+} in oxides. If M^{5+} ions in the $NaMO_3$ lattice are replaced with Ir ions, Ir^{4+} ions and oxygen defects should form to maintain the charge balance according to the formula of

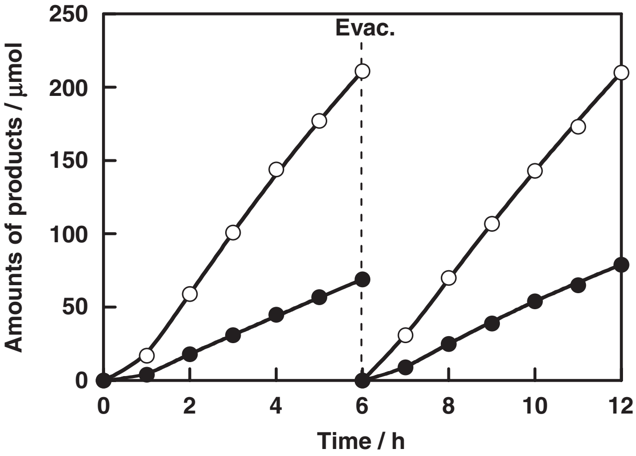

Figure 1. Photocatalytic water splitting over pretreated (R773–O473) NiO(0.5 wt %)/$NaNbO_3$. R773–O473 indicates the pretreatment of H_2-reduction at 773 K for 2 h and O_2-oxidation at 473 K for 1 h. Open mark: H_2, closed marks: O_2. Catalyst: 0.3 g, pure water: 350 mL, light source: 400-W high-pressure Hg lamp, reaction cell: inner irradiation cell made of quartz.

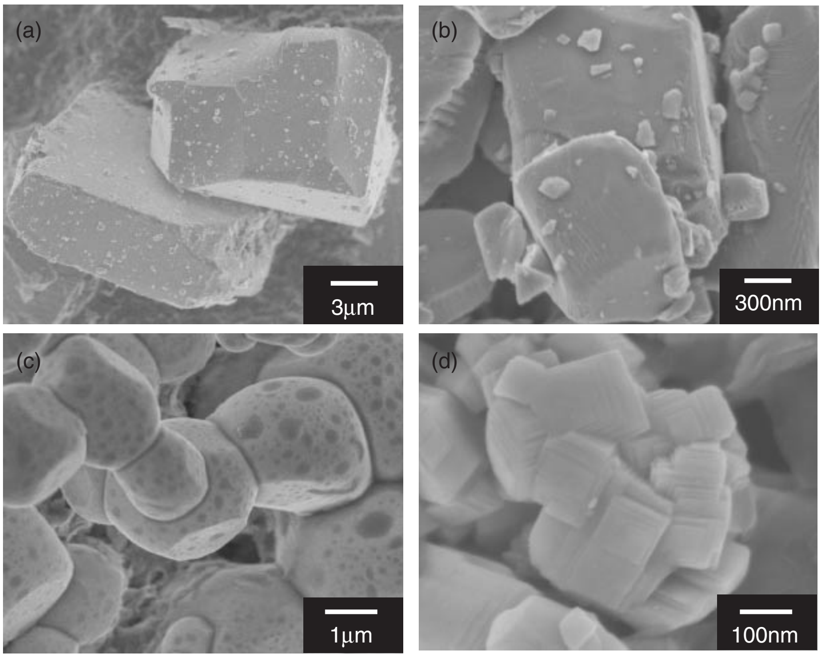

Figure 2. SEM images of (a) $NaNbO_3$:Ir(0.1%), (b) $NaNbO_3$:Ir(0.1%)/Sr(0.5%), (c) $NaTaO_3$:Ir(1%), and (d) $NaTaO_3$:Ir(1%)/La(2%).

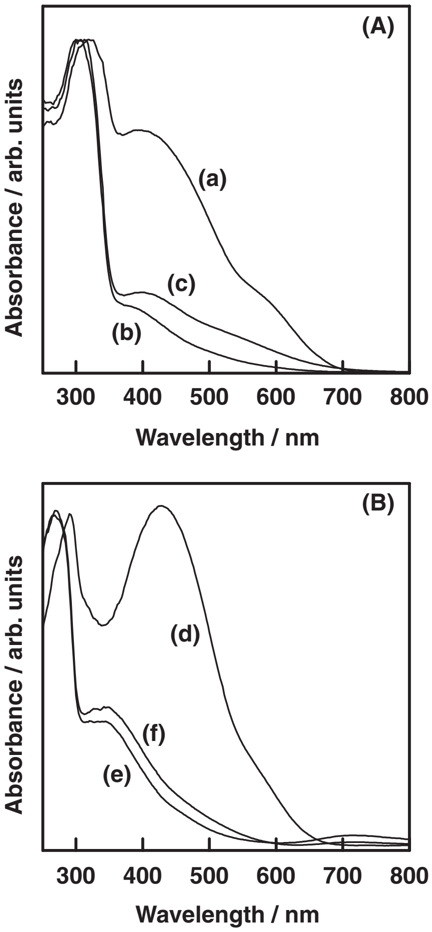

Figure 3. Diffuse reflectance spectra of (A) $NaNbO_3$:Ir(0.1%)/Sr(x%) and (B) $NaTaO_3$:Ir(1%)/La(y%). (a) $x = 0$, (b) $x = 0.5$, and (c) $x = 0.5$ with H_2-reduction at 473 K, (d) $y = 0$, (e) $y = 2$, and (f) $y = 2$ with H_2-reduction at 473 K.

Table 1. Photocatalytic H_2 and O_2 Evolution over Ir-Doped $NaNbO_3$ and $NaTaO_3$ from Aqueous Solutions Containing Sacrificial Reagents under Visible Light Irradiation[a)]

Photocatalyst	Dopant /mol %	EG /eV	SA /$m^2\,g^{-1}$	Activity/μmol h^{-1}	
				H_2[b)]	O_2[c)]
$NaNbO_3$	Ir(0.1)	1.8, 2.1	0.7	0.9	0
$NaNbO_3$	Ir(0.1)/Sr(0.5)	1.8–1.9	1.8	11	4.8
$NaNbO_3$	Ir(0.1)/Ba(0.5)	1.8–1.9	2.0	10	2.8
$NaNbO_3$	Ir(0.1)/La(0.5)	1.8–1.9	1.9	5.3	3.0
$NaTaO_3$	Ir(1)	1.9, 2.2	0.4	0	0
$NaTaO_3$	Ir(1)/Sr(2)	2.1–2.3	3.4	7.5	0
$NaTaO_3$	Ir(1)/Ba(2)	2.1–2.3	3.3	4.5	0
$NaTaO_3$	Ir(1)/La(2)	2.1–2.3	3.3	11	0

a) Catalyst: 0.3 g, reactant solution: 120 mL, light source: 300-W Xe-lamp with a cutoff filter (L42), reaction cell: top-irradiation cell with Pyrex window. b) Pt(0.3 wt %) co-catalyst, 10 vol % of an aqueous methanol solution. c) 0.02 mol L^{-1} of an aqueous $AgNO_3$ solution.

$NaM^{V}{}_{1-2x}Ir^{IV}{}_{2x}O_{3-x}$. Therefore, it was considered that these visible-light absorption bands shown in Figures 3A-a and 3B-d were mainly due to electronic transition associated with Ir^{4+}. On the other hand, Ir^{3+} ions that make electron donor levels were mainly formed without the formation of oxygen defects to keep the charge balance by codoping of alkaline earth metal and lanthanum ions according to the following schemes.

$$Na^{I} + Nb^{V} \text{ or } Ta^{V} \rightarrow La^{III} + Ir^{III} \quad (1)$$

$$2Na^{I} + Nb^{V} \text{ or } Ta^{V} \rightarrow 2A^{II} + Ir^{III} \quad (2)$$

When strontium or lanthanum ions were codoped into $NaMO_3$:Ir, the visible light absorption bands became smaller as shown in Figures 3A-b and 3B-e. The absorption edge of $NaTaO_3$:Ir/La was positioned at shorter wavelength than that of $NaNbO_3$:Ir/Sr mainly due to the difference in the conduction band between $NaNbO_3$ and $NaTaO_3$. Both absorption bands were assigned to the electronic transition from electron donor levels formed with Ir^{3+} to conduction bands composed of Nb4d or Ta5d orbitals. On the other hand, the visible light absorption band of $NaNbO_3$:Ir was similar to that of $NaTaO_3$:Ir, because they were assigned to the electronic transition from the valence band composed of O2p orbitals to the electron acceptor levels formed with Ir^{4+}. As a result, the peak and the onset positions of the visible light absorption band of $NaTaO_3$:Ir were different from those of $NaTaO_3$:Ir/La. The intensities of the visible light absorption bands of $NaMO_3$:Ir/A were slightly increased by H_2-reduction as shown in Figures 3A-c and 3B-f. The absorption bands of the codoped samples were mainly due to Ir^{3+}-related electronic transition. However, the increase in the intensity by H_2-reduction suggested that a small amount of Ir^{4+} ions still existed even after the codoping. Although excess amounts of codopants were added compared with theoretical ratios as shown in schemes 1 and 2 in order to maintain the charge balance sufficiently for the samples in Figure 3, the formation of Ir^{4+} ions was not completely suppressed.

The authors have previously reported codoping effects for TiO_2:Ni/Ta,[3] TiO_2:Cr/Sb,[4] TiO_2:Rh/Sb,[5] and $SrTiO_3$:Cr/Ta[7] photocatalysts. The charge balance was kept by substitution of dopant–codopant pairs for the same site as Ti^{4+} in these photocatalysts, whereas it was maintained by substitution of the dopant–codopant pairs for different A and B sites of perovskite structure in the present case of Ir-doped $NaMO_3$ (M: Nb and Ta).

Table 1 lists photocatalytic activities of $NaMO_3$:Ir (M: Nb and Ta) and $NaMO_3$:Ir/A (A: Sr, Ba, and La). A typical time course of hydrogen evolution is also shown in Figure 4. $NaMO_3$ doped with only Ir hardly gave H_2 from an aqueous methanol solution, whereas codoped photocatalysts steadily produced H_2 under visible light irradiation after an induction period of about one hour. The appearances of the photocatalytic activities by the codoping were due to the suppression of the formation of recombination centers between photogenerated electrons and holes such as Ir^{4+} and/or oxygen defects, as shown in schemes 1 and 2. The small particle size and high surface area of photocatalyst powder obtained by doping of alkaline earth metal ions and lanthanum ions also contributed to the appearances of photocatalytic activities, as shown in Figure 2. Strontium and lanthanum were the most effective codopants for Ir-doped $NaNbO_3$ and $NaTaO_3$, respectively. Moreover, the codoped $NaNbO_3$ possessed photocatalytic

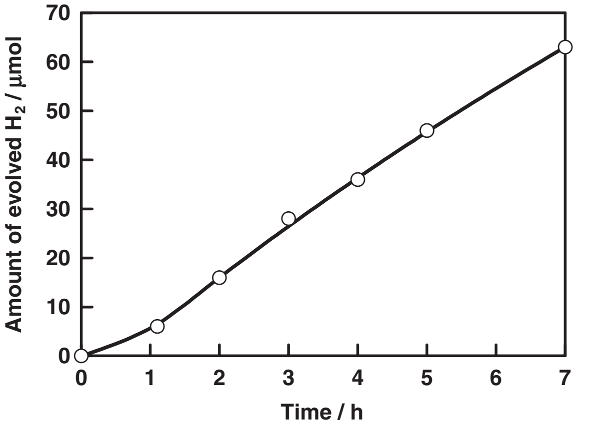

Figure 4. Photocatalytic H_2 evolution from an aqueous methanol solution (10 vol %) over Pt(0.3 wt %)/$NaNbO_3$:Ir(0.1%)/Sr(0.5%) under visible light irradiation. Catalyst: 0.3 g, reactant solution: 120 mL, light source: 300-W Xe-lamp with a cutoff filter (L42), reaction cell: top-irradiation cell with Pyrex window.

activity for O_2 evolution from an aqueous silver nitrate solution under visible light irradiation. In contrast, the codoped $NaTaO_3$ did not show activity for O_2 evolution. The electron donor level formed with partially filled 5d orbitals of Ir^{3+} in $NaTaO_3$:Ir/La would be more negative (0.1–0.4 eV) than that in $NaNbO_3$:Ir/Sr, judging from the differences in the conduction band level between $NaNbO_3$ and $NaTaO_3$ (0.6 eV) and in the energy gap between $NaNbO_3$:Ir/Sr and $NaTaO_3$:Ir/La (0.2–0.5 eV). Therefore, $NaTaO_3$:Ir/La had lower driving force for oxidation of H_2O to produce O_2 than $NaNbO_3$:Ir/Sr. This is one of the reasons for the difference in the ability of O_2 evolution between $NaNbO_3$:Ir/Sr and $NaTaO_3$:Ir/La.

Figure 5 shows diffuse reflectance spectra after photocatalytic H_2 evolution and the wavelength dependency of H_2 evolution for Pt(0.3 wt %)/$NaNbO_3$:Ir(0.1%)/Sr(0.5%) and Pt(0.3 wt %)/$NaTaO_3$:Ir(1%)/La(2%). The wavelength of incident light was controlled with cutoff filters. Although the diffuse reflectance spectra after photocatalytic H_2 evolution were similar not to original spectra but to spectra after H_2-reduction shown in Figure 3, except for higher base lines due to loaded Pt-cocatalysts. Actually, the color of the photocatalyst changed from originally subdued cream color to bright cream color during the photocatalytic H_2 evolution. The color of photocatalyst after the reaction was similar to that with H_2-reduction. These changes in color and the observation of an induction period for H_2 evolution indicated that a small amount of Ir^{4+} ions remained as suggested from Figure 3. The remaining Ir^{4+} ions were reduced to Ir^{3+} by the photo-excited electrons at the early stage of the reaction. The energy gaps of photo-reduced $NaNbO_3$:Ir(0.1%)/Sr(0.5%) and $NaTaO_3$:Ir(1%)/La(2%) were estimated to be 1.8 and 2.1 eV, respectively. The onsets of the wavelength dependency of the H_2 evolution agreed well with those of diffuse reflectance spectra of the samples after the reaction. These results indicated that H_2 evolved with electronic transition from the electron donor levels formed with partially filled 5d orbitals of Ir^{3+} to the conduction bands composed of Nb4d or Ta5d. Thus, it was found that codoped $NaNbO_3$ and $NaTaO_3$ showed photocatalytic activities for H_2 or O_2 evolution from an aqueous solution containing a sacrificial reagent under visible light irradiation.

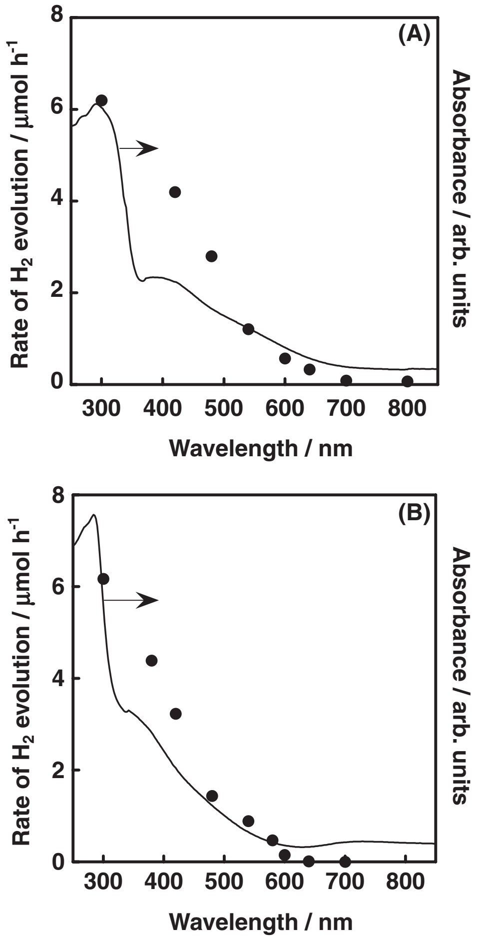

Figure 5. Wavelength dependencies of H_2 evolution (closed circles) from an aqueous methanol solution (10 vol %) and diffuse reflectance spectra of (A) Pt(0.3 wt %)/$NaNbO_3$:Ir(0.1%)/Sr(0.5%) and (B) Pt(0.3 wt %)/$NaTaO_3$:Ir(1%)/La(2%) after H_2 evolution. Catalyst: 0.1 g, reactant solution: 120 mL, light source: 300-W Xe lamp with cutoff filters.

Conclusion

Oxidation numbers of iridium substituted for Nb^{5+} and Ta^{5+} ions at B sites of perovskite structure for $NaNbO_3$ and $NaTaO_3$ were controlled by codoping of alkaline earth metal and lanthanum ions for Na^{+} ions at A sites. $NaNbO_3$:Ir/A (A: Sr, Ba, and La) showed H_2 or O_2 evolution, while $NaTaO_3$:Ir/A showed H_2 evolution under visible light irradiation. Diffuse reflectance spectra of $NaMO_3$:Ir/A (M: Nb and Ta) revealed that the photocatalytic H_2 evolution proceeded accompanied by electronic transition from the electron donor level formed with partially filled 5d orbitals of Ir^{3+} to the conduction band composed of Nb4d or Ta5d orbitals. The Ir^{3+} species were formed by codoping of Sr^{2+}, Ba^{2+}, and La^{3+} and photogenerated electrons at the beginning stage of H_2 evolution. The doping of iridium will be an effective strategy for development of new visible-light-responsive photocatalysts not only for H_2 evolution but also for O_2 evolution employing wide band gap photocatalysts as hosts.

This work was supported by a Grant-in-Aid (No. 20037061) for Priority Area Research (No. 460) from the Ministry of Education, Culture, Sports, Science and Technology. One of us (A.I.) has been awarded a Research Fellowships of the Japan Society for the Promotion of Science for Young Scientists.

References

1 A. Kudo, R. Niishiro, A. Iwase, H. Kato, *Chem. Phys.* **2007**, *339*, 104, and references therein.

2 A. Kudo, Y. Miseki, *Chem. Soc. Rev.* **2009**, *38*, 253, and references therein.

3 R. Niishiro, H. Kato, A. Kudo, *Phys. Chem. Chem. Phys.* **2005**, *7*, 2241.

4 H. Kato, A. Kudo, *J. Phys. Chem. B* **2002**, *106*, 5029.

5 R. Niishiro, R. Konta, H. Kato, W.-J. Chun, K. Asakura, A. Kudo, *J. Phys. Chem. C* **2007**, *111*, 17420.

6 R. Konta, T. Ishii, H. Kato, A. Kudo, *J. Phys. Chem. B* **2004**, *108*, 8992.

7 T. Ishii, H. Kato, A. Kudo, *J. Photochem. Photobiol., A* **2004**, *163*, 181.

8 H. Kato, K. Asakura, A. Kudo, *J. Am. Chem. Soc.* **2003**, *125*, 3082.

9 A. Iwase, H. Kato, H. Okutomi, A. Kudo, *Chem. Lett.* **2004**, *33*, 1260.

10 K. Domen, S. Naito, M. Soma, T. Onishi, K. Tamaru, *J. Chem. Soc., Chem. Commun.* **1980**, 543.

11 K. Domen, A. Kudo, T. Onishi, N. Kosugi, H. Kuroda, *J. Phys. Chem.* **1986**, *90*, 292.

12 G. Li, T. Kako, D. Wang, Z. Zou, J. Ye, *J. Phys. Chem. Solids* **2008**, *69*, 2487.

13 R. D. Shannon, *Acta Crystallogr., Sect. A* **1976**, *32*, 751.